



## OPEN

## Origin of cold bias over the Arabian Sea in Climate Models

S. Sandeep &amp; R. S. Ajayamohan

Center for Prototype Climate Modeling, New York University Abu Dhabi, UAE.

## SUBJECT AREAS:

ATMOSPHERIC SCIENCE

OCEAN SCIENCES

Received

4 June 2014

Accepted

29 August 2014

Published

17 September 2014

Correspondence and  
requests for materials  
should be addressed to  
R.S.A. (Ajaya.  
Mohan@nyu.edu)

Almost all climate models in Coupled Model Inter-comparison Project phase five (CMIP5) were found to have a cold bias in Sea Surface Temperature (SST) over the northern Arabian Sea, which is linked to the biases in the Indian Summer Monsoon (ISM). This cold SST bias was attributed to the anomalous cold winds from the north-western part of south Asian landmass during boreal winter. However, the origin of the anomalously strong cold winds over the Arabian Sea and its association with the large-scale circulation is obscure. Here we show that an equatorward bias in subtropical Jetstream during boreal spring season anomalously cools down the northern Arabian Sea and adjoining land regions in CMIP5 models. The models with stronger equatorward bias in subtropical jet are also the ones with stronger cold SST bias over the Arabian Sea. The equatorward shift coupled with enhanced strength of the subtropical jet produce a stronger upper tropospheric convergence, leading to a subsidence and divergence at lower levels over the Arabian deserts. The low entropy air flowing from the Arabian land mass cools the northern Arabian Sea. The weaker meridional temperature gradients in the colder models substantially weaken ISM precipitation.

The Sea Surface Temperature (SST) biases are arguably the most prominent error in Coupled General Circulation Model (CGCM) simulations<sup>1</sup>, which can result in amplification of model error due to the feedback between different components of climate system<sup>2</sup>. Experiments with Atmospheric General Circulation Models coupled to prescribed SSTs shows that the external radiative forcing do not directly warm up the continents; rather it warms up the oceans which in turn results in a continental warming<sup>3</sup>. This suggests that SST biases can have far reaching impact on the simulation of continental climate<sup>4,5</sup>. Thus understanding the origins of SST bias is important to improve the model simulations. Tropics-wide bias in SSTs in the fifth phase of Coupled Model Inter-comparison Project<sup>6</sup> (CMIP5) models has been traced to biases in the simulations of clouds and thermocline depth by the coupled models<sup>7</sup>. Both the local and large-scale oceanic and atmospheric processes are dominant elements for the SST biases<sup>8–10</sup> in various ocean basins. Understanding the factors responsible for SST biases specific to different ocean basins are vital as those aid climate modelers to rectify these biases. In this context, finding the origin of SST biases over the Indian Ocean assumes significance. Further, such an analysis also helps in gaining in-depth understanding on the interdependence of various fields in a climate model.

The ocean-atmosphere coupling is very important for the existence of Indian Summer Monsoon (ISM) and to maintain its inter-annual and intra-seasonal variability<sup>11,12</sup>. Further, precipitation in the monsoon region is sensitive to the tropical SSTs<sup>13,14</sup>. An accurate simulation of the ISM precipitation is still a challenge to the current generation CGCMs<sup>15,16</sup>, with the Arabian Sea SST cold bias during the pre-monsoon season highlighted as a major reason for the land precipitation error<sup>17–19</sup>. The anomalous cold winds from the north-west India and adjoining land regions in the CGCMs are suggested as the cause of anomalous cooling of Arabian Sea SSTs<sup>18</sup>. The cold SSTs over the Arabian Sea can reduce the meridional temperature gradients that drive the monsoon circulation. However, the model mechanisms that cause anomalous cooling of air over south Asian land mass in the pre-monsoon season are not yet clear. One possible explanation is that, inadequately resolved orography west of Tibet may cause dry air intrusion which is linked to a thermodynamic bias in ISM simulated by many CGCMs<sup>20</sup>. An equatorward latitudinal bias in the eddy driven jetstreams in the Southern Hemisphere is identified as a common problem in many CGCMs<sup>21</sup>, which is attributed to the biases in midlatitude cloud forcing<sup>22</sup>. Further, asymmetric warming between the hemispheres can anomalously shift both Inter-Tropical Convergence Zone (ITCZ) and jetstreams towards warmer hemisphere<sup>23</sup>. The double ITCZ, a longstanding problem associated with most of the CGCMs, is found to be a response to the increased Southern Hemispheric shortwave forcing<sup>24</sup>.

Although the equatorward bias in the eddy driven jetstreams and ITCZ are known issues in CGCMs, the presence of such biases in the Sub-Tropical Jetstreams (STJ) are not clear. During boreal winter and spring

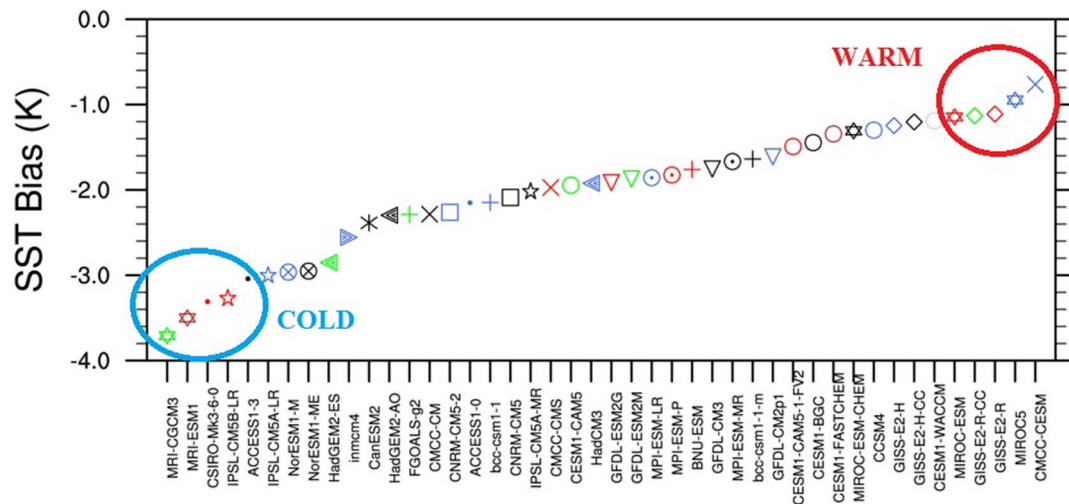


**Figure 1 | Arabian Sea SST bias.** Northern Arabian Sea ( $15^{\circ}\text{N}$ – $25^{\circ}\text{N}$ ;  $60^{\circ}\text{E}$ – $70^{\circ}\text{E}$ ) spring season (March – May) SST bias (K) calculated for 44 CMIP5 models. The bias in historical all forcing simulations are computed with reference to fifty year (1951–2000) climatology of HadISST1.1. This figure is plotted using NCAR Command Language (NCL).

seasons STJ core is located around  $30^{\circ}\text{N}$  which recedes to north of  $\sim 40^{\circ}\text{N}$  by the beginning of the summer, in tune with the ISM onset<sup>25</sup>. It is possible that the inadequately resolved orography west of the Tibetan Plateau in some models<sup>20</sup> may also cause a southward shift of STJ over the Southeast Asia. The cold dry air associated with STJ can cool the South Asian land mass and the adjacent oceans during pre-monsoon season. The anomalous cooling over the ocean can persist even after the STJ moves north prior to monsoon onset, owing to the higher heat capacity of the ocean. The persisting cold anomaly over the northern Indian Ocean can hamper the development of monsoon in its early phase. However, the role of such large-scale circulation biases in producing anomalously cold SSTs in the Arabian Sea is not examined.

Here we explore the pre-monsoon SST bias over the Arabian Sea in CMIP5 historical simulations. We specifically investigate the possible presence of an equatorward bias in STJ, in the wake of known biases in ITCZ and eddy driven jets<sup>23,24</sup>.

## Results

All 44 CMIP5 coupled models (see X axis in Fig. 1) analyzed here exhibit cold SST bias over the northern Arabian Sea during pre-monsoon season (March – May; Fig. 1). The magnitudes of cold SST bias in the models range between 0.5 and 3.8 K, consistent with the previous analysis<sup>18</sup>. The pre-monsoon climatology of the surface temperatures from ERA Interim (ERA-I) reanalysis<sup>26</sup> shows Arabian Sea SSTs in 299 – 302 K range. A composite of five less cold (WARM; Fig. 2b) models show slightly cooler SSTs over the Arabian Sea, ranging between 298 and 302 K. The composite of five coldest (COLD; Fig. 2c) models simulate much colder SSTs. The difference between COLD and WARM models clearly shows a strong negative gradient in SST over the northern Arabian Sea (Fig. 2d). The contrast in surface temperature is even stronger over the land mass adjoining the Arabian Sea. The ERA-I land surface temperature over the north-west India and Arabian deserts exceeds 308 K in the pre monsoon season (Fig. 2a). Both the WARM and COLD models simulate colder

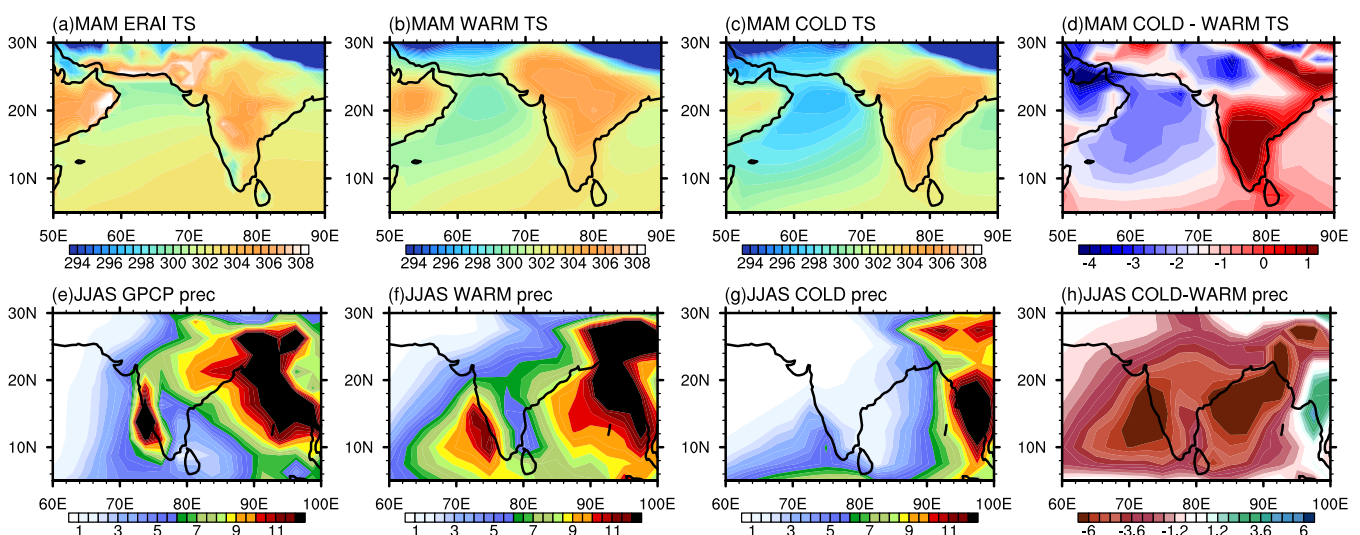


**Figure 2 | Pre-monsoon surface temperature and monsoon precipitation.** Climatological (MAM) surface temperature (K) from (a) ERAI, (b) WARM composite, (c) COLD composites, and (d) difference between COLD and WARM model composites; climatological (JJAS) precipitation ( $\text{mm day}^{-1}$ ) from (e) GPCP, (f) WARM and (g) COLD model composites and (h) difference between WARM and COLD models. WARM and COLD models are indicated in Fig. 1. GPCP precipitation climatology is calculated for 1980–2009 period. All other calculations are based on 1951–2000 period. This figure is plotted using NCL.



land surface compared to the observations, with the latter showing stronger cooling. The development of ISM circulation is critically dependent on the land-sea temperature contrast<sup>11</sup>. The observed June – September (JJAS) precipitation (Fig. 2e) shows strong orographic precipitation band over the Western Ghats and Arakan mountains. The precipitation pattern in WARM models (Fig. 2f) is comparable with the observations, although the models simulate less precipitation over the Western Ghats. Also, the precipitation band extends to northwest India in the WARM models as in observations. In the COLD models (Fig. 2g), the JJAS precipitation is substantially weaker all over the Southeast Asia compared to WARM composite and the precipitation band has not reached northwestern parts of India. The difference between COLD and WARM composites (Fig. 2h) clearly reveals the weak precipitation in the former, in line with previous analysis<sup>19</sup>. This suggests that negative surface temperature gradients in the COLD models might have slowed down the advancement of monsoon circulation. It is worth noting that none of the CMIP5 models has been successful in simulating all features of ISM satisfactorily<sup>15,16</sup>, in line with the cold SST bias. Identifying the processes responsible for pre-monsoon cold SST bias may have far reaching implications towards an improved model performance of ISM simulation. So far, the investigations on cold SST bias are centered around local processes, like advection of the cold winds from northwest India and Pakistan during boreal winter and spring seasons<sup>17,18</sup>. However, these studies stop short of explaining the origin of anomalous cold air over Asian land mass during boreal winter and spring.

A main circulation feature over the subtropics is the STJ, which is a response to the equator-pole atmospheric temperature gradient<sup>27</sup>. Typically STJ recedes to north of about 40°N during boreal summer, in tune with the onset of ISM<sup>25</sup>. The difference in 200 hPa zonal winds between COLD and WARM models (Fig. 3a) demonstrate that the COLD models have the core of the jet located much closer to the equator than WARM models. Over the northern Arabian Sea, wind speed at 200 hPa exceeds 8 m s<sup>-1</sup> in COLD models when compared to the WARM composite. A comparison with ERAI reanalysis (Fig. 3b) shows that, the STJ core in COLD models is located equatorward (see blue dot in Fig. 3b) of both ERAI and WARM models. Further, STJ core is shifted vertically downward toward higher pressure level when compared to the ERAI STJ location. In contrast, the STJ core in WARM models is located upward of its climatological position in ERAI. Further, the strength of STJ core is overestimated (slightly underestimated) in COLD (WARM) models, with maximum wind speeds of 41 m s<sup>-1</sup> (34 m s<sup>-1</sup>) as compared to ERAI wind speed of ~36 m s<sup>-1</sup>. The core of STJ is located at 30°N at an altitude of 175 hPa in ERAI. The mean position of STJ core in WARM (COLD) models is located at 29.5°N and 160 hPa (27.7°N and 190 hPa). A latitude-height view of the COLD-WARM zonal mean zonal winds (Fig. 3c) clearly shows that the equatorward bias in the zonal winds in COLD models is not confined to upper levels, but exists throughout the depth of the troposphere.

The prevalence of strong cold air advection over the Arabian Sea can result in anomalous cooling of SSTs in COLD models. In order to verify the relation between the anomalous STJ and SST bias over the Arabian Sea, a correlation analysis between the climatological (1951–2000) zonal winds at 500 hPa and SST bias is carried out for the MAM season (Fig. 4a). Both the winds and SSTs are area averaged over 15°N–25°N and 60°E–70°E, where the strongest cold anomaly is seen over the Arabian Sea. A strong correlation of -0.74 is obtained between the two parameters, further strengthening our argument that the STJ and pre-monsoon Arabian Sea SST bias are related. It is rather straightforward to elucidate the cause-effect relationship between the biases in STJ and Arabian Sea SST. Since STJ is a planetary scale feature, and the equatorward bias in the COLD models span around the globe, it is safe to argue that the SST bias over a small region like Arabian Sea may not cause the bias in STJ. On the

other hand, the analyses presented so far indicate that the bias in Arabian Sea SST is most likely linked to the STJ biases.

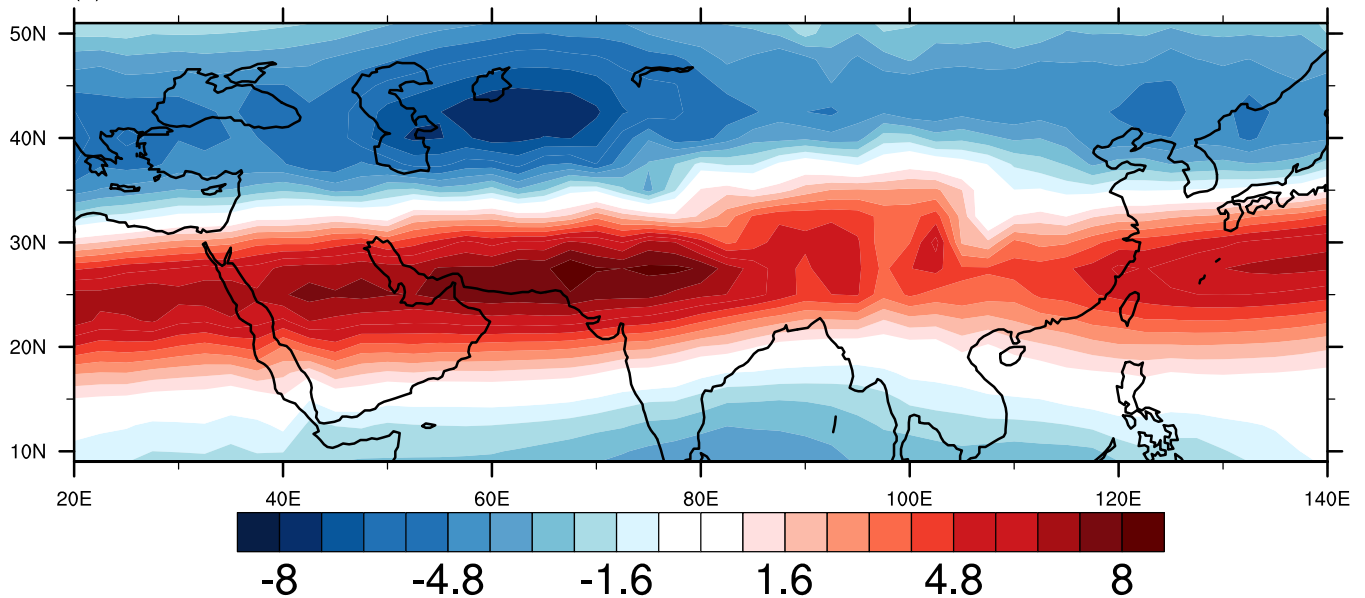
The STJ is located on the poleward flanks of the Hadley Cell (HC) and the distance between the two STJs on both sides of the equator may be considered as a measure of the width of the tropics<sup>28</sup>. The composite climatology of the zonal mean meridional mass stream function ( $\chi$ ) in WARM models shows the descending branch of the HC between 5 and 25°N, with its core positioned around mid-troposphere (Fig. 4b). On the other hand the HC in the COLD composite has a broader and shallow descending structure that spans between Equator and 25°N, (Fig. 4c), consistent with the slightly downward location of the maxima of STJ (see Fig. 3b). In order to bring out the covariability of HC and STJ locations in model simulations, a linear regression of the zonal mean zonal winds on the poleward edge latitude of HC ( $\Phi_{HC}$ ) across all models is performed (Fig. 4d; see methods for details). The poleward latitude of HC is taken as the latitude at which  $\chi$  at 500 hPa becomes zero in the northern hemisphere. The COLD (WARM) models are found to have a mean value of  $\Phi_{HC} = 25.5^\circ\text{N}$  (27.1°N). The latitude-height structure of the regression slope indicate that the models in which HC subsidence occur at more southward latitude also have the westerly wind maxima located more equatorward. The negative (positive) values of regression slopes show linear relationship between increased (decreased) westerly winds and more equatorward (poleward) latitude of HC subsidence. Thus the model-to-model variance in the location of STJ maxima is explained by that of  $\Phi_{HC}$ . A thermodynamic bias over the ISM region in climate models was suggested to be linked to inadequately resolved orography over north-western part of India<sup>20</sup>. However, the effect of model resolution on the bias in STJ in CMIP5 simulations is not clear. It may be noted that MRI-CGCM3, which is one of the highest resolution (1.125°×1.125°) models in CMIP5, has the strongest pre-monsoon SST bias (see Fig. 1).

How does the equatorward shift in the STJ produce cold SST bias over the Arabian Sea? The mechanism that couples shift in STJ location and cooling of the Arabian Sea is explained in Fig. 5. STJ causes an upper level positive vorticity, as shown in Fig. 5a, in which the MAM climatological composite wind vectors and relative vorticity at 250 hPa for the WARM models is depicted. The stronger winds and its possible interaction with the orography due to a southward shift of STJ cause stronger relative vorticity in COLD models (Fig. 5b). The difference between COLD and WARM models clearly shows a stronger upper level convergence over a large region north of the Arabian Sea in COLD models (Fig. 5c). The upper level convergence can induce a subsidence which in turn produces a divergence at lower levels. This mechanism is very clear with weak divergence at 850 hPa in WARM models (Fig. 5d) and strong divergence in COLD models (Fig. 5e). The larger values of geopotential height in COLD models indicate stronger subsidence at lower levels, as compared to WARM models. The low level subsidence location is found to be southwest of the upper level convergence area, which may be due to the orographic forcing just beneath the upper tropospheric convergence region. The difference between COLD and WARM composites shows stronger subsidence and divergence at 850 hPa over the Arabian Peninsula and a stronger southward wind flow over the Arabian Sea in COLD models (Fig. 5f). This mechanism explains the origin of anomalous wind flow over the Arabian Sea in COLD models during pre-monsoon period. The wind vectors and equivalent potential temperature ( $\theta_e$ ) at 925 hPa show low entropy advection towards Arabian Sea in WARM composite (Fig. 6a). The advection of low entropy air in COLD models is substantially stronger and intrudes further south over the Arabian Sea (Fig. 6b). This low level advection of dry and cold air over the Arabian Sea can cool the sea surface. Thus the southward shift in the STJ can explain the cooling of northern Arabian Sea SST in CMIP5 models.

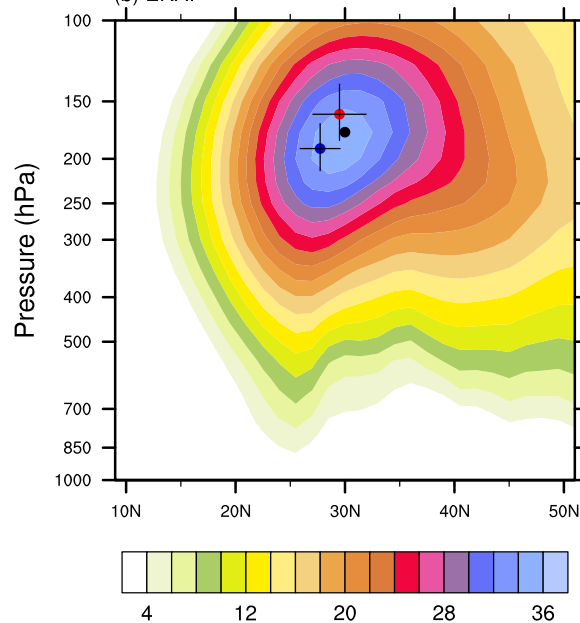




(a) COLD - WARM U200hPa



(b) ERAI



(c) COLD - WARM

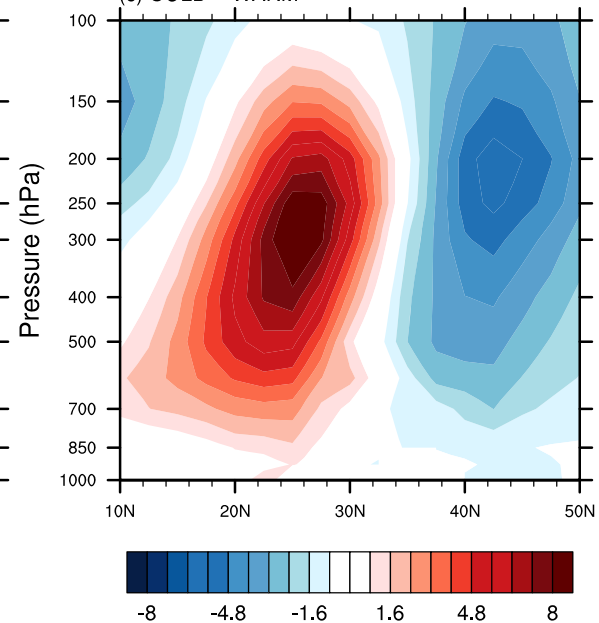


**Figure 3 | Horizontal and vertical structure of zonal winds.** (a) Difference between COLD and WARM model composites for zonal winds ( $\text{m s}^{-1}$ ) at 200 hPa. (b) Latitude – height cross-section of zonal mean ( $50^{\circ}\text{E}$ – $100^{\circ}\text{E}$ ) zonal winds from ERA-Interim reanalysis; the red (blue) dots show the mean location of jet core in WARM (COLD) models and the vertical and horizontal lines indicate the standard deviation of the core locations. The mean latitude of STJ core in WARM (COLD) models is  $29.5^{\circ}\text{N} \pm 2.4^{\circ}$  ( $27.7^{\circ}\text{N} \pm 1.8^{\circ}$ ). The mean altitude of STJ core in WARM (COLD) models is  $160 \pm 22.4$  ( $190 \pm 22.4$ ) hPa. The mean  $\pm$  standard deviation of jet core speed in WARM (COLD) models is  $34 \pm 3.5$  ( $41 \pm 3.9$ )  $\text{m s}^{-1}$ . The black dot represents the core of jet in ERAI ( $30^{\circ}\text{N}$  and 175 hPa). The mean jet core speed of ERAI is  $36 \text{ m s}^{-1}$ ; (c) Latitude – height cross-section of COLD – WARM model composites of zonal mean zonal winds. All calculations are done using fifty years (1951–2000) climatological mean spring season, except in the case of ERAI, for which thirty year (1980–2009) climatology is used. This figure is plotted using NCL.

## Discussion

We have presented a mechanism that explains the Arabian Sea cold SST bias during pre-monsoon season in many CGCMs. The current understanding on the issue tries to attribute the Arabian Sea cold SST bias to the anomalous cold air advection from northwest India and adjoining land regions. However, these investigations fall short of identifying the source of anomalous cooling of continental air over the Asian land mass. It is important to understand the exact cause of the SST bias in order to improve the performance of the CGCMs.

Our analysis finds that the origin of anomalously cold air over the South Asian land mass in CGCMs originates from a southward shift coupled with increased strength of the STJ. The biases in the location and strength of STJ are explained by the location of northern hemispheric Hadley Cell subsidence. The biases in the strength and location of Hadley Cell subsidence may be linked to the biases in the radiative forcing<sup>24</sup>. Our results demonstrate the linkage between the large-scale circulation and a local phenomenon at a relatively smaller ocean basin and the resultant impact on regional climate. The biases

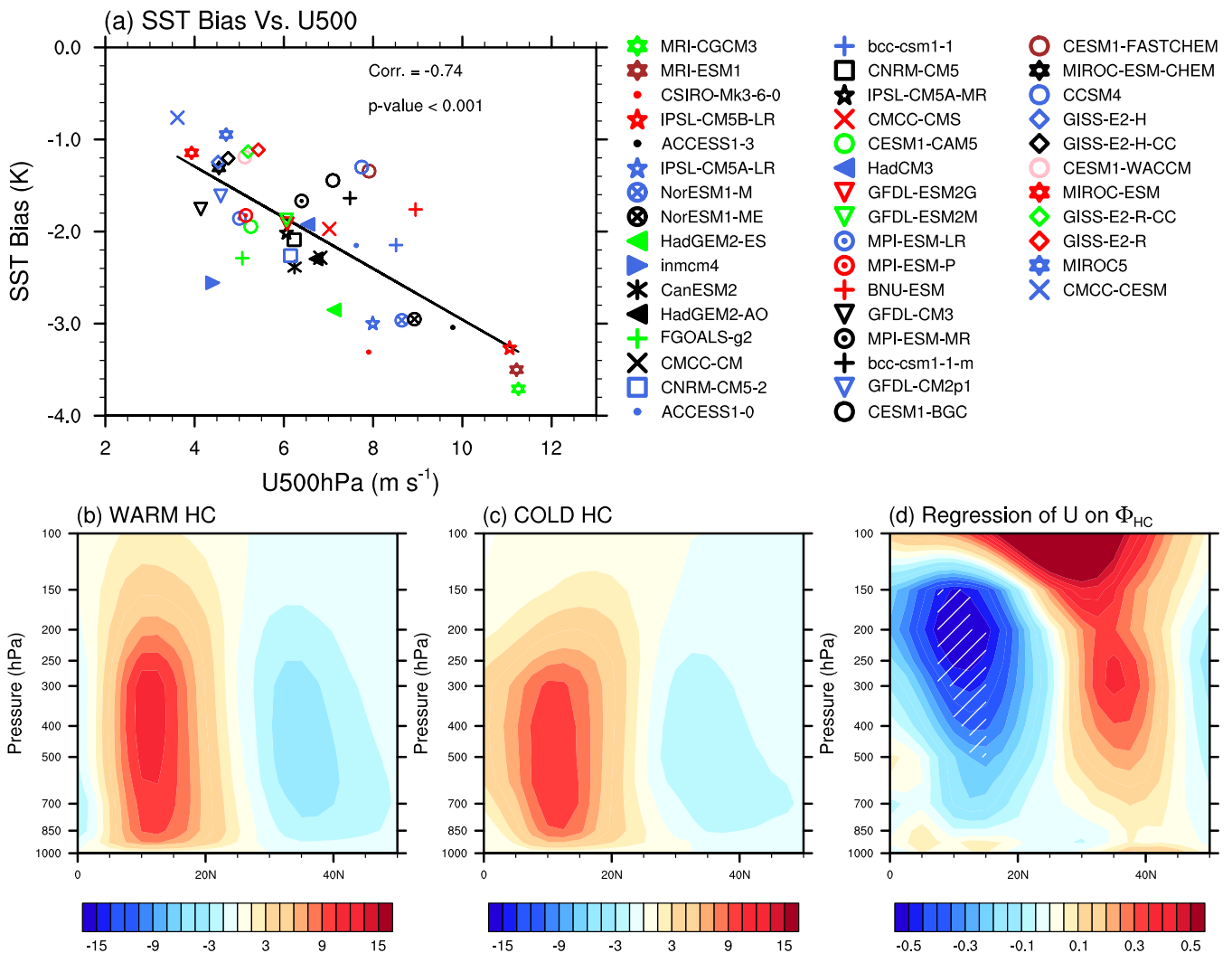


**Figure 4 | Wind speed versus SST bias.** (a) Scatter plot between area averaged (15°N–25°N and 60°E–70°E) 500 hPa zonal wind (m s<sup>-1</sup>) and northern Arabian Sea SST bias (K) during March – May Season; Hadley Cell and zonal winds. (b) WARM and (c) COLD model composites of zonal mean stream function (10<sup>10</sup> kg s<sup>-1</sup>); (d) linear regression of Hadley Cell latitude on zonal mean (50°E–100°E) zonal winds during March - May season. Stippling in (d) shows statistically significant ( $p < 0.05$ ) regression slopes as revealed by a two-tailed  $t$ -test. This figure is plotted using NCL.

in SST and STJ are found to be independent of the temporal scale used for the calculations (see methods for details). Since the summer monsoon precipitation influences the life of the entire South Asian continent with a massive population, prediction of monsoon rainfall assumes significance. The results in this study help to identify the cause of the most prominent systematic bias seen in climate models in simulating the seasonal mean monsoon precipitation.

## Methods

We used monthly mean outputs of CMIP5 historical all forcing simulations. The period during 1951–2000 is used for the calculations presented here. The fifty year climatology is sufficient to address the natural variability of various temporal frequencies. Our focus is pre-monsoon season, as the strong ocean-atmosphere coupling during monsoon season makes it difficult to attribute the SST bias to a source other than the coupled processes. The Hadley Center Sea Surface Temperature<sup>29</sup> (HadISST1.1) is used to calculate the SST bias in CMIP5 models. The observation density in HadISST1.1 in the second half of the 20<sup>th</sup> century is better compared to the first half<sup>29</sup>, which is the reason we choose 1951–2000 as the base period for our calculations. However, in order to ensure robustness, the calculations are repeated for another two temporal scales (not shown here) – entire 20<sup>th</sup> century and 1981–2000 period. All the three temporal scales chosen for the analysis yielded identical results, suggesting that the biases are independent of temporal scale. The surface temperature form model output is used as a proxy for model SST. The SST bias is computed over the Arabian Sea region of 15°N–25°N and 60°E–70°E. The zonal mean of the zonal winds are computed over the longitudes 50°E–100°E. The zonal winds from ERA-Interim (ERA-I) reanalysis<sup>26</sup> are used for qualitative comparison of the model

simulated zonal winds. Also the surface temperature from ERA-I is used to compare with the model simulated surface temperature. The Global Precipitation Climatology<sup>30</sup> version 2.2 (GPCP) monthly precipitation data is used to compare the model simulated precipitation. All the model data are interpolated to a common 2.5°×2.5° latitude-longitude grid using linear interpolation, before doing calculations.

The core of subtropical Jetstream is calculated in a way identical to the technique proposed to calculate the core of mid-latitude Jetstream<sup>31</sup>. The latitudinal location of the core of the jet,  $\phi_{jet} = \frac{\int_{U \geq U_x} \phi U(\phi) d\phi'}{\int_{U \geq U_x} U(\phi) d\phi'}$ ; where  $\phi$  is the latitude,  $U_x$  is a threshold value of the zonal mean (50°E–100°E) zonal winds ( $U$ ) around the jet core, over which the integral is calculated. Here  $U_x$  is defined as  $U_x = 0.9U_{max}$  where  $U_{max}$  is the maximum zonal wind at the jet core (grid point maximum). The structure of the jet is symmetric closer to the core and becomes asymmetric away from it (see Fig. 3b). The value of  $U_x$  should be taken in such a way that the integral is calculated over a symmetric curve around  $U_{max}$ . Otherwise this method may produce a bias in the calculation of the  $\phi_{jet}$ . The advantage of calculating  $\phi_{jet}$  using this method rather than taking the latitude of  $U_{max}$  is that we can overcome the issue of coarse grid resolution.

The regression slope in Fig. 4d is calculated as follows. Regression coefficient at a particular grid point,  $\beta = \left( \frac{1}{n} \sum U_i U_i^T \right)^{-1} \left( \frac{1}{n} \sum U_i \phi_i \right)$ ; where  $U$  denotes zonal wind at a grid point,  $\phi$  the poleward latitudinal boundary of northern hemispheric Hadley Cell, the subscript  $i$  stands for the index of CMIP5 models (span from 1 to 43) and ' $n$ ' for total number of models used in the calculation (in this case  $n=43$ ). It may be noted that the three dimensional monthly mean wind data are not available for the model CESM1-CAM5-1-FV2 (historical experiment) in CMIP5 archive while carrying out this study, and hence omitted in the regression analysis. The models are

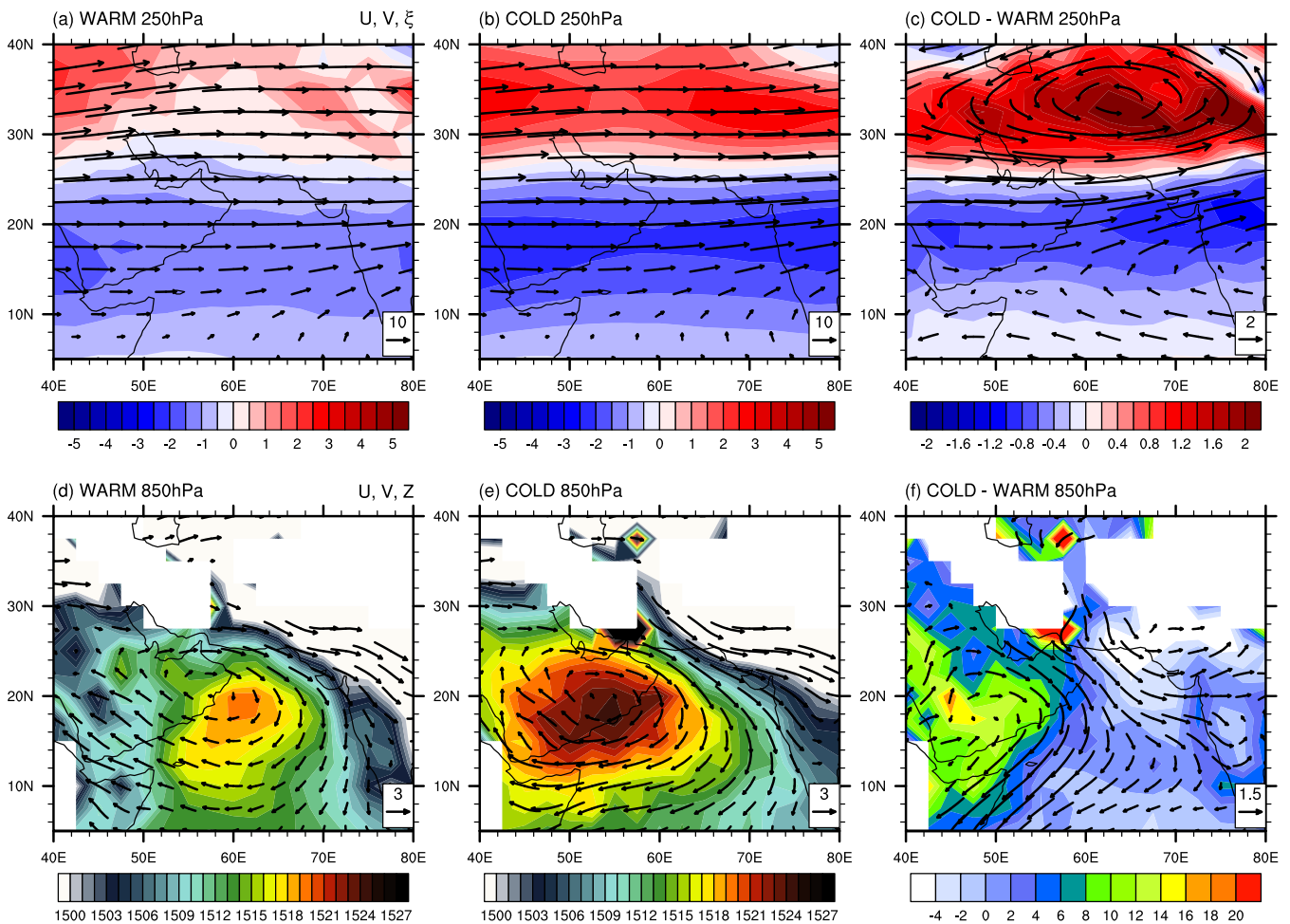


**Figure 5 | Upper level convergence and lower level divergence.** Wind vector ( $m s^{-1}$ ) and relative vorticity ( $10^{-5} s^{-1}$ ) at 250 hPa for (a) WARM, (b) COLD model composites, and (c) difference between COLD and WARM model composites; wind vector and geopotential height (m) at 850 hPa for (d) WARM, (e) COLD model composites, and (f) difference between COLD and WARM model composites. This figure is plotted using NCL.

organized in alphabetical order of their names. The poleward latitude of HC is the latitude at which  $\chi$  at 500 hPa becomes zero. This calculation is carried out for each latitude-height grid cell to generate the regression map. This regression map explains the relation between model-to-model variability in the zonal mean zonal winds and

the latitude of Hadley Cell subsidence. Two tailed *t*-test is used to identify the values of regression slopes that are statistically significant at 5% level ( $P$ -value  $< 0.05$ ).

**Graphics software:** All plots are produced with NCAR Command Language.

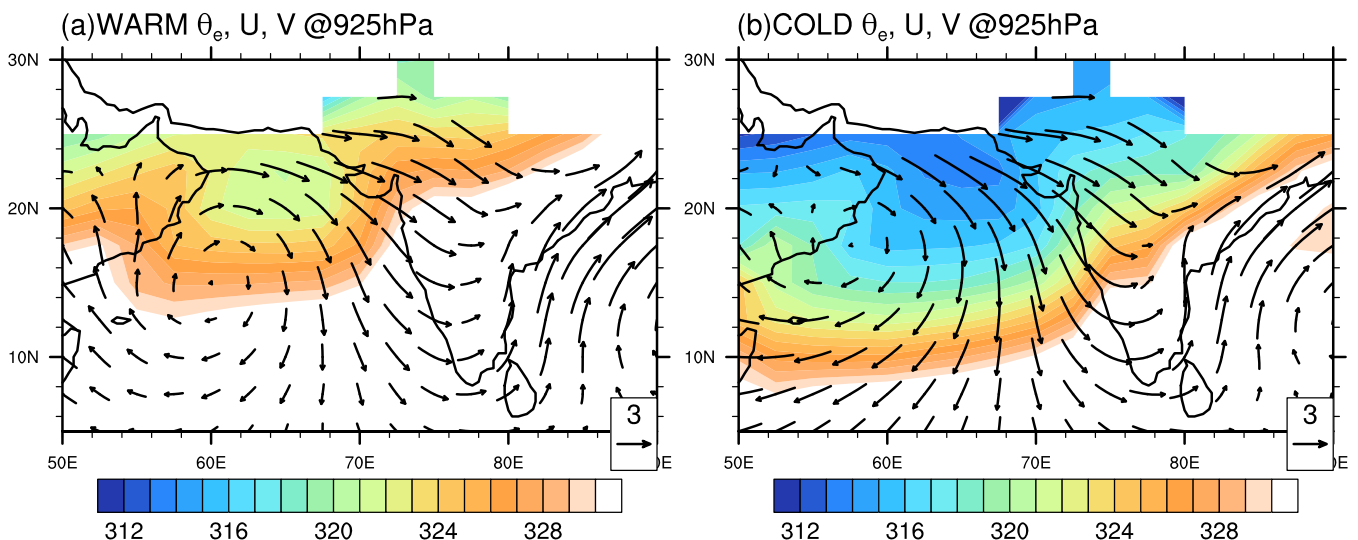


**Figure 6 | Intrusion of low entropy air.** Climatological  $\theta_e$  (K) and wind vector ( $m s^{-1}$ ) composites at 925 hPa for (a) WARM and (b) COLD models. 1951–2000 MAM climatology is used. This figure is plotted using NCL.



1. Large, W. G. & Danabasoglu, G. Attribution and Impacts of Upper-Ocean Biases in CCSM3. *J. Clim.* **19**, 2325–2346, doi:10.1175/JCLI3740.1 (2006).
2. Cai, W., Sullivan, A., Cowan, T., Ribbe, J. & Shi, G. Simulation of the Indian Ocean Dipole: A relevant criterion for selecting models for climate projections. *Geophys. Res. Lett.* **38**, doi:10.1029/2010gl046242 (2011).
3. Compo, G. P. & Sardeshmukh, P. D. Oceanic influences on recent continental warming. *Clim. Dyn.* **32**, 333–342, doi:10.1007/s00382-008-0448-9 (2008).
4. Ashfaq, M., Skinner, C. & Diffenbaugh, N. Influence of SST biases on future climate change projections. *Clim. Dyn.* **36**, 1303–1319, doi:10.1007/s00382-010-0875-2 (2011).
5. Keeley, S. P. E., Sutton, R. T. & Shaffrey, L. C. The impact of North Atlantic sea surface temperature errors on the simulation of North Atlantic European region climate. *Quart. J. Roy. Meteor. Soc.* **138**, 1774–1783, doi:10.1002/qj.1912 (2012).
6. Taylor, K. E., Stouffer, R. J. & Meehl, G. A. An Overview of CMIP5 and the Experiment Design. *Bull. Am. Meteorol. Soc.* **93**, 485–498, doi:10.1175/BAMS-D-11-00094.1 (2011).
7. Li, G. & Xie, S.-P. Origins of tropical-wide SST biases in CMIP multi-model ensembles. *Geophys. Res. Lett.* **39**, L22703, doi:10.1029/2012GL053777 (2012).
8. Vannière, B., Guilyardi, E., Toniazzo, T., Madec, G. & Woolnough, S. A systematic approach to identify the sources of tropical SST errors in coupled models using the adjustment of initialised experiments. *Clim. Dyn.*, doi:10.1007/s00382-014-2051-6 (2014).
9. Xu, Z., Li, M., Patricola, C. & Chang, P. Oceanic origin of southeast tropical Atlantic biases. *Clim. Dyn.* 1–16, doi:10.1007/s00382-013-1901-y (2013).
10. Toniazzo, T. & Woolnough, S. Development of warm SST errors in the southern tropical Atlantic in CMIP5 decadal hindcasts. *Clim. Dyn.* 1–25, doi:10.1007/s00382-013-1691-2 (2013).
11. Webster, P. J. & Fasullo, J. in *Encyclopedia of Atmospheric Sciences* (eds Holton, J. & Curry, J. A.) 1370–1386 (Academic Press, 2003).
12. Ajayamohan, R. S., Rao, S. A. & Yamagata, T. Influence of Indian Ocean Dipole on poleward propagation of boreal summer intraseasonal oscillations. *J. Clim.* **21**, 5437–5454, doi:10.1175/2008JCLI1758.1 (2008).
13. Roxy, M. Sensitivity of precipitation to sea surface temperature over the tropical summer monsoon region—and its quantification. *Clim. Dyn.*, doi:10.1007/s00382-013-1881-y (2013).
14. Sabin, T. P., Babu, C. A. & Joseph, P. V. SST-convection relation over tropical oceans. *Int. J. Climatol.* **33**, 1424–1435, doi:10.1002/joc.3522 (2013).
15. Sperber, K. R. *et al.* The Asian summer monsoon: an intercomparison of CMIP5 vs. CMIP3 simulations of the late 20th century. *Clim. Dyn.* **41**, 2711–2744, doi:10.1007/s00382-012-1607-6 (2013).
16. Ramesh, K. V. & Goswami, P. Assessing reliability of regional climate projections: the case of Indian monsoon. *Sci. Rep.* **4**, doi:10.1038/srep04071 (2014).
17. Levine, R. C., Turner, A. G., Marathayil, D. & Martin, G. M. The role of northern Arabian Sea surface temperature biases in CMIP5 model simulations and future projections of Indian summer monsoon rainfall. *Clim. Dyn.* **41**, 155–172, doi:10.1007/s00382-012-1656-x (2013).
18. Marathayil, D., Turner, A. G., Shaffrey, L. C. & Levine, R. C. Systematic winter sea-surface temperature biases in the northern Arabian Sea in HiGEM and the CMIP3 models. *Environ. Res. Lett.* **8**, 014028, doi:10.1088/1748-9326/8/1/014028 (2013).
19. Levine, R. C. & Turner, A. G. Dependence of Indian monsoon rainfall on moisture fluxes across the Arabian Sea and the impact of coupled model sea surface temperature biases. *Clim. Dyn.* **38**, 2167–2190, doi:10.1007/s00382-011-1096-z (2011).
20. Boos, W. R. & Hurley, J. V. Thermodynamic Bias in the Multimodel Mean Boreal Summer Monsoon. *J. Clim.* **26**, 2279–2287, doi:10.1175/JCLI-D-12-00493.1 (2012).
21. Barnes, E. A. & Hartmann, D. L. Testing a theory for the effect of latitude on the persistence of eddy-driven jets using CMIP3 simulations. *Geophys. Res. Lett.* **37**, L15801, doi:10.1029/2010GL044144 (2010).
22. Ceppi, P., Hwang, Y.-T., Frierson, D. M. W. & Hartmann, D. L. Southern Hemisphere jet latitude biases in CMIP5 models linked to shortwave cloud forcing. *Geophys. Res. Lett.* **39**, doi:10.1029/2012gl053115 (2012).
23. Ceppi, P., Hwang, Y.-T., Liu, X., Frierson, D. M. W. & Hartmann, D. L. The relationship between the ITCZ and the Southern Hemispheric eddy-driven jet. *J. Geophys. Res.* **118**, 5136–5146, doi:10.1002/jgrd.50461 (2013).
24. Hwang, Y.-T. & Frierson, D. M. W. Link between the double-Intertropical Convergence Zone problem and cloud biases over the Southern Ocean. *Proc. Nat. Acad. Sci.*, doi:10.1073/pnas.1213302110 (2013).
25. Goswami, B. N. in *Intraseasonal Variability in the Atmosphere-Ocean Climate System* (eds Lau, W. K. M. & Waliser, D. E.) 19–61 (Springer, 2005).
26. Dee, D. P. *et al.* The ERA-Interim reanalysis: configuration and performance of the data assimilation system. *Quart. J. Roy. Meteor. Soc.* **137**, 553–597, doi:10.1002/qj.828 (2011).
27. Galvin, J. F. P. The weather and climate of the tropics Part 2 –The subtropical jet streams. *Weather* **62**, 295–299, doi:10.1002/wea.65 (2007).
28. Seidel, D. J., Fu, Q., Randel, W. J. & Reichler, T. J. Widening of the tropical belt in a changing climate. *Nat. Geosci.* **1**, 21–24 (2008).
29. Rayner, N. A. *et al.* Global analyses of sea surface temperature, sea ice, and night marine air temperature since the late nineteenth century. *J. Geophys. Res.* **108**, 4407, doi:10.1029/2002jd002670 (2003).
30. Huffman, G. J., Adler, R. F., Bolvin, D. T. & Gu, G. Improving the global precipitation record: GPCP Version 2.1. *Geophys. Res. Lett.* **36**, doi:10.1029/2009gl040000 (2009).
31. Ceppi, P., Zelinka, M. D. & Hartmann, D. L. The response of the Southern Hemispheric eddy-driven jet to future changes in shortwave radiation in CMIP5. *Geophys. Res. Lett.* **41**, 3244–3250, doi:10.1002/2014GL060043 (2014).

## Acknowledgments

The Center for Prototype Climate Modeling is fully funded by the Government of Abu Dhabi through New York University Abu Dhabi (NYUAD) Research Institute grant. This work was carried out on NYUAD HPC resources.

## Author contributions

S.S. conceived the idea. S.S. and R.S.A. designed the analysis. S.S. plotted figures. Both S.S. and R.S.A. contributed to writing the manuscript.

## Additional information

**Competing financial interests:** The authors declare no competing financial interests.

**How to cite this article:** Sandeep, S. & Ajayamohan, R.S. Origin of cold bias over the Arabian Sea in Climate Models. *Sci. Rep.* **4**, 6403; DOI:10.1038/srep06403 (2014).



This work is licensed under a Creative Commons Attribution-NonCommercial-NoDerivs 4.0 International License. The images or other third party material in this article are included in the article's Creative Commons license, unless indicated otherwise in the credit line; if the material is not included under the Creative Commons license, users will need to obtain permission from the license holder in order to reproduce the material. To view a copy of this license, visit <http://creativecommons.org/licenses/by-nc-nd/4.0/>